Research Square

Preprints are preliminary reports that have not undergone peer review.
They should not be considered conclusive, used to inform clinical practice,
or referenced by the media as validated information.

Foliar fungal endophyte communities remain unaltered under urban air-pollution but differentially express stress-related genes

Valeria Stephany Flores-Almaraz
Universidad Nacional Autónoma de México
Camille Truong
Royal Botanic Gardens Victoria
Diana Hernández-Oaxaca
Universidad Nacional Autónoma de México
Verónica Reyes-Galindo
Universidad Nacional Autónoma de México
Alicia Mastretta-Yanes
Consejo Nacional de Humanidades Ciencias y Tecnología (CONAHCYT)
Juan Pablo Jaramillo-Correa
Universidad Nacional Autónoma de México
Rodolfo Salas-Lizana (rsalas@ciencias.unam.mx)
Universidad Nacional Autónoma de México

Research Article

Keywords: metatranscriptomics, metabarcoding, oxidative stress, tropospheric ozone, foliar endophytes, Abies religiosa

Posted Date: December 23rd, 2023

DOI: https://doi.org/10.21203/rs.3.rs-3761022/v1

License: This work is licensed under a Creative Commons Attribution 4.0 International License. Read Full License

Additional Declarations: No competing interests reported.

Abstract

Air pollution caused by tropospheric ozone contributes to the decline of forest ecosystems; for instance, coniferous forests dominated by sacred fir, *Abies religiosa* (Kunth) Schltdl. & Cham., in the peri-urban forests of Mexico City. Individual trees within these forests exhibit variation in their response to ozone exposure, such as the presence or absence of visible symptoms in needles. Using RNA-Seq metatranscriptomic data and ITS2 metabarcoding, we investigated whether such symptom variation correlates with the taxonomic and functional composition of fungal endophytes from needles collected in a highly polluted area in the surroundings of Mexico City. Our findings indicate that ozone-related symptoms do not significantly correlate with changes in the taxonomic composition of fungal endophytes. However, 21 putative proteins were differentially expressed in fungal endophytes from asymptomatic needles, including eight genes previously associated with resistance to oxidative stress. These results suggest that fungal endophyte communities likely play a role in mitigating the oxidative burst caused by tropospheric ozone to sacred fir. Our study illustrates the feasibility of using RNA-Seq data, accessible from global sequence repositories of plants, for the characterization of fungal endophyte communities and gene expression.

Introduction

Tropospheric ozone (O_3) is a serious threat to human health, biodiversity and ecosystem function [1]. Although the effects of O_3 on plants have been widely studied [2], the impacts of O_3 on fungal endophytes and interactions with stressed host plants are poorly understood. Fungal endophytes are plant-inhabiting fungi that do not produce symptoms of colonization in their host for most of their life cycle [3]. Fungal endophytes exhibit a broad spectrum of life-history strategies, from parasitic to mutualistic [4]. When acting as mutualists, fungal endophytes can enhance their host fitness when they face biotic and abiotic stresses [5], including oxidative stress [6].

The taxonomic and functional composition of fungal endophytes can be affected by several biotic and abiotic stressors. For example, fungal pathogens and bacteria can cause the regreening of senescent leaf tissues in *Acer* while reducing the overall fungal richness and altering leaf fungal communities [7], although such changes differ among *Acer* species. In contrast, fungal endophyte communities are not correlated with pathogenic symptoms in *Vanilla* or *Eucalyptus* plants affected by pathogenic fungi and a wasp, respectively [8, 9]. However, in the case of *Eucalyptus* plants, differentially expressed genes associated with secondary metabolism and fungal biomass were observed in resistant and susceptible plants, respectively [8]. Regarding O_3 stress, Liu et al. [10] found a general decrease in overall fungal richness and an increase in pathogenic fungi abundance in plants experimentally exposed to high levels of O_3. Other studies have suggested that fungal endophytes may minimize the extent of damage caused by O_3 to their plant hosts by directly secreting antioxidant agents or by inducing the activation of plant antioxidants [11]. However, no study so far has investigated the effect of O_3 on the gene expression of fungal endophytes.

Tropospheric ozone is particularly harmful in heavily populated cities, like Mexico City. The geographic location and topography of Mexico City, which is situated above 2,200 m asl and encircled by mountains in three directions, concentrate high amounts of O_3 for extended periods of time [12], exacerbating its detrimental effects on urban and peripheral forests [13, 14]. Air pollutants drain across the surrounding mountains,

particularly toward the southwest, where forests of the conifer sacred fir (*Abies religiosa* (Kunth) Schltdl. & Cham.) dominate the native vegetation (Fig. 1a-b). In regions such as the Desierto de los Leones National Park, situated ca. 30 km southwest of Mexico City, O_3 concentrations can be as high as 117 ppb between March and June (the dry-warm season) [12]. These values exceed by five times the recommended level for safeguarding forest trees [15]. In these forests, observed symptoms related to O_3 stress include leaf chlorosis, needle casting, branch loss, and eventually death [16].

Sacred fir is a native coniferous tree to central and southern Mexico and western Guatemala [19], where it forms monodominant forests (Fig. 1a-b). These forests represent one of the few remaining forested areas in the vicinity of Mexico City that provide ecosystem services, such as erosion control, carbon sequestration and water retention [20]. Most of the remaining forests are conserved within Desierto de los Leones National Park, Santa Rosa Xochiac communal land and other local communities territories [21]. Visible signs of O_3 damage initially appear as faint whitish spots on the upper surface of needles, gradually coalescing and developing into larger lesions with brownish-red coloration [22] (Fig. 1c-b). Despite the elevated O_3 levels at Desierto de los Leones National Park, visible needle symptoms can vary among individuals, with some displaying symptoms in several, but not all, branches while others remain completely asymptomatic [22]. The presence of visible symptoms was later associated with decreased terpenoid accumulation and distinct gene expression patterns associated with the response to various abiotic and biotic stresses [23].

Responses to O_3 stress have been extensively documented in plants [24]. However, a comprehensive understanding of the physiological effects of O_3 on plant-associated fungal endophyte communities, as well as its impact on the interactions between plants and their associated mycobiota, have not been fully elucidated. Several studies on the effects of O_3 on fungi have focused on its use as an antifungal agent for seed sterilization and for controlling contamination caused by *Aspergillus*, *Penicillium*, and *Rhizopus* [25, 26]. The antifungal effect of O_3 is attributed to its ability to increase fungal cell membrane permeability, induce damage to fungal cell walls, and thereby alter lipid, carbohydrate, and protein metabolism [26]. These alterations ultimately lead to the excessive accumulation of reactive oxygen species (ROS) and death [25].

RNA-seq data is an increasingly important tool for plant studies on development, stress response, and biotic interactions, among others [27, 28]. RNA extracted from plant tissues most likely contains RNA from the associated microbiome (fungi and bacteria), allowing the study of the gene expression of plant microbiomes [29]. For example, Chialva et al. [30] mined previously generated RNA-Seq data from tomato plants to infer the taxonomy and function of the root microbiota. In this study, we characterized fungal communities and fungal gene expression from O_3-related symptomatic and asymptomatic *A. religiosa* needles using ITS2 metabarcoding and plant RNA-Seq data generated by Reyes-Galindo [23]. We hypothesized that 1) the presence of visible O_3-associated symptoms is correlated with changes in the taxonomic composition of fungal communities within *A. religiosa* needles, leading to a reduction in foliar endophyte species richness and relative abundance, along with a simultaneous increase in pathogenic taxa richness and relative abundance; and 2) fungal endophytes present in asymptomatic needles differentially express genes associated with antioxidant mechanisms. Finally, we evaluated whether RNA-Seq data targeting host plants could provide significant taxonomic and functional information about the endophytic fungal communities of these plants.

Methods

Sampling and data generation

Samples used in this study were previously collected and processed by Reyes-Galindo [23]. Briefly, we collected samples from the Santa Rosa Xochiac community (19.285 N, 99.301 W), in the buffer zone of the Desierto de los Leones National Park, southwestern Mexico City, in May 2017.

We selected this area due to the elevated mortality rate of *A. religiosa* individuals, which can be attributed to a combination of factors including air pollution, drought, nutritional deficiencies, insect pathogens, and a lack of forest management after recurrent anthropogenic forest fires [31]. We sampled individuals 10–15 years old within an area of approximately 1 ha. We selected five individuals with reddish needles (i.e., symptomatic) and five other individuals without visible symptoms. We collected symptomatic needles (Fig. 1c) from symptomatic trees and asymptomatic needles (Fig. 1d) from asymptomatic trees. In both cases we collected needles situated on branches from the previous two growth seasons (2015 and 2016). Needles were preserved in RNAlater (Sigma–Aldrich) and stored at -70°C until processing.

We extracted total RNA from 40–45 mg of plant tissue using the Spectrum RNA Plant Kit (SIGMA) and evaluated its integrity via 1% agarose gel electrophoresis. The quality and purity of the RNA were determined using a NanoDrop spectrophotometer based on the 260/280 and 260/230 ratios. Quantification of the RNA concentration was performed using the Qubit RNA assay (Invitrogen). Library construction was performed through mRNA enrichment by polyadenylated RNA capture (polyA-capture), retrotranscription, and subsequent sequencing using a HiSeq 4000 150×2 paired-end protocol (Illumina). The library preparation and sequencing procedures were carried out at the University of Berkeley, USA. Demultiplexing was performed by the sequencing service.

DNA was extracted from 80 mg of tissue ground with liquid nitrogen using a DNeasy Plant Mini Kit (QIAGEN), following the manufacturer's protocol. We amplified the ITS2 region of nuclear rDNA using the fungal-specific primers gITS7ngs and ITS4ngsUNI [32] with the Platinum PCR SuperMix High Fidelity Kit (Invitrogen). PCR conditions were as follows: initial denaturation at 94°C for 1 min, followed by 35 cycles at 94°C for 30 s, 52°C for 30 s, 68°C for 30 s, and a final extension step at 68°C for 7 min. We constructed Amplicon libraries with Nextera adapters (Illumina), which were normalized at equimolar concentrations, purified with Agencourt AMPure XP beads (Beckman) and sequenced using a MiSeq 300×2 paired-end protocol (Illumina) at the University of Arizona Genetics Core, USA.

ITS2 metabarcoding

We ‘denoised’ the sequences and clustered them into operational taxonomic units (OTUs) at 97% similarity using the AMPtk 1.3.0 pipeline [33] following Bermúdez-Contreras et al. [34]. OTU taxonomy was assigned in AMPtk by aligning reference sequences with the UNITE database [35]. We used negative and positive controls according to Nguyen et al. [36]. We removed OTU occurrences that accounted for < 0.5% of sequence counts per sample to eliminate potential sequencing artifacts. To account for the variation in the number of ITS2 reads per sample, we transformed read counts into relative abundances by averaging the number of reads per sample, multiplying them by 1000 and transforming them to the next integer, which was used as counts [37].

RNA-Seq metatranscriptomics

We used *Abies religiosa* RNA-Seq data generated from Reyes-Galindo [23]. We removed low quality reads and adapters using Trimmomatic v0.39 [38] and verified read quality using FastQC v0.11.8 [39] and MultiQC v1.0.dev0 [40]. We removed the host reads by mapping the reads to the *Abies balsamea* transcriptome (GenBank Accession: GGJG00000000, Bioproject: PRJNA437248) using the BWA-MEM software [41]. We then assembled both paired and unpaired reads that did not map to the reference transcriptome into contigs using SPAdes v3.13.0 [42], and estimated assembly statistics with QUAST v5.0.2 [43].

Additionally, to maximize the number of assembled genes for functional analyses, we produced five *de novo* assemblies using host-filtered RNA-Seq reads from all samples: one with rnaSPAdes v3.13.0 [42] with default parameters, and four with Trinity v2.8.5 [44], using the parameters specified in Table S1. We evaluated assembly quality, by measuring the number of genes and isoforms with RSEM v1.3.3 [45], and assembly length with metaquast v3.2 [46]; we then selected the assembly providing the highest number of assembled genes, isoforms, and total length.

To assign taxonomy to RNA-Seq reads, we implemented two widely used algorithms in shotgun metagenomic studies for fungal taxonomic classification: Kraken2 v.2.1.2-Bracken [47, 48] and Kaiju v1.8.0 [49]. We used the RefSeq database, limiting the search parameters to complete fungal genomes/proteins, and performed both analyses using high-quality filtered reads and contigs separately. We evaluated the performance of both algorithms and data types by counting the number of identified taxa at each taxonomic rank and comparing them to the number of identified taxa using ITS2 metabarcoding. The database-algorithm combination with the smallest ratio of unique taxa was selected for further analyses.

Taxonomic profiling

We characterized and visualized fungal communities in R v4.0.2 [50] using the phyloseq [51], ggvenn v0.1.9 [52], microbiome v1.13.12. [53], vegan v2.5-7 [54], eulerr v6.1.1 [55], ggplot2 v3.4.2 [56], DESeq2 v.40.1 [57], indicspecies v1.7.13 [58] and Ampvis2 v2.8.3 [59] packages. Putative fungal endophytes and plant pathogens were assigned to OTUs based on FungalTraits [60] using the "Foliar endophyte" (Endophytic interaction capability) and "Plant pathogenic capacity" annotations. We tested for differences in community observed richness between datasets (ITS2 metabarcoding or RNA-Seq metatranscriptomics), needle conditions (symptomatic or asymptomatic), and guilds (foliar endophyte or plant pathogen). These analyses were carried out using generalized linear models with a Poisson distribution. To test for differences in guild relative abundance between needle condition and dataset, we used a generalized linear model with a binomial distribution. Fungal community composition was visualized using nonmetric multidimensional scaling (NMDS) with Raup–Crick distances, based on OTU presence/absence, after eliminating OTUs that were present in only one sample. Differences in community composition between datasets and conditions were tested with a PERMANOVA with 9999 permutations.

To evaluate if there was an association between specific OTU relative abundances and host needle condition, we calculated the indicator value index (IndVal) [61] with the multipatt function in indicspecies. To assess differences in relative abundance among fungal classes between conditions, we calculated the

log2FoldChange using the symptomatic condition as reference and conducted a Wald test with adjusted *p-values* for multiple comparisons, as implemented in DESeq2.

Functional profiling

We predicted open reading frames (ORFs) with Transdecoder v.5.5.0 [62] annotated them with eggNOG-mapper v2 [63] against the eggNOG 5.0 database [64]. We estimated transcription levels by mapping host-filtered reads to predicted ORFs using Salmon v1.8.0 [65] and imported them into R v4.0.2 using the tximport package [66]. We visualized the functional composition of each sample by evaluating the relative abundance of all COG categories assigned to each ORF using ggplot2 and performed differential expression analyses with DESeq2 [57], using samples of symptomatic needles as reference. We evaluated statistically significant differences in $\log_2$FoldChange using the Wald test as implemented in DESeq2.

Custom scripts for all analyses performed are available at
https://github.com/valeriafloral/Abies_fungal_endophytes

Results

Taxonomic profiling

ITS2 metabarcoding produced 59,698–156,065 reads per sample that clustered into 259 OTUs. In turn, between 89.2% and 95.8% of the quality-filtered RNA-Seq reads matched to *A. religiosa* which, after removal, yielded 12,500,000–21,200,000 nonhost reads per sample; these were assembled into 4,988–20,572 contigs per sample. The Kraken2-Bracken algorithm yielded 24,108–105,092 nonhost reads and 1,485–5,545 contigs that were taxonomically classified into 86 OTUs. The Kaiju algorithm allowed the identification of more taxa, for a total of 482 OTUs detected from contigs and 484 from reads (Fig. S1) but also produced a higher ratio of uniquely identified taxa than Kraken2-Bracken (Fig. S2). For subsequent analyses we therefore selected the dataset from Kraken2-Bracken (reads).

Diversity analyses

A greater number of OTUs was detected when using ITS2 metabarcoding (n = 259) than when using RNA-Seq metatranscriptomics (n = 86). Both methods further retrieved different numbers of taxa at each taxonomic level; indeed, the two datasets barely overlapped, sharing no species, one genus, five families, five orders, five classes and two phyla (Fig. 2a). Based on NMDS ordination and PERMANOVA, we found that the dataset used (RNA-Seq metatranscriptomics or DNA metabarcoding) was significantly correlated with differences in fungal community composition ($R^2 = 1$, *p-value* = 0.001), whereas needle condition remained non-significant (Fig. 2b).

We found that each dataset retrieved a different number of fungal classes (15 for ITS2 metabarcoding and nine for RNA-Seq metatranscriptomics). Nevertheless, both datasets shared five classes that presented the highest relative abundances, including Dothideomycetes, Eurotiomycetes, and Sordariomycetes (Fig. 3). Although no significant differences in fungal class relative abundances were found between needle conditions in any dataset, class Leotiomycetes exhibited a marginally significant increase in asymptomatic needles (*p value* = 0.06). Using the ITS2 metabarcoding dataset, we observed a significantly greater relative abundance of two OTUs in asymptomatic needles, identified as Lecanorales sp. (IndVal = 0.89, *p value* = 0.048) and

Phaeomoniella sp. (IndVal = 0.89, *p value* = 0.047), both within Ascomycota. On the other hand, we found no significant differences in the relative abundance of any OTU between needle conditions when using the RNA-Seq metatranscriptomic dataset.

Regarding guilds, we identified 20 OTUs corresponding to foliar endophytes and 78 OTUs corresponding to plant pathogens in the ITS2 metabarcoding dataset. Likewise, using the RNA-Seq metatranscriptomic dataset, we identified 17 OTUs as foliar endophytes and 85 OTUs as plant pathogens. We found no differences in the observed richness between samples from symptomatic and asymptomatic needles for the entire fungal community or for putative fungal endophytes or plant pathogens (Fig. 4a and c). However, the observed richness was significantly different between datasets for all fungi (β = -0.19, *p-value* = 0.003), plant foliar endophytes (β = 0.78, *p-value* < 0.001) and plant pathogens (β = 0.31, *p-value* = 0.036). We also found that regardless of the needle condition and dataset, plant pathogen richness was significantly greater than foliar endophyte richness (β = 0.8, *p-value* < 0.001).

We did not find differences in the relative abundance of putative foliar endophytes or plant pathogens between samples from symptomatic and asymptomatic needles. However, we did find significant differences between datasets (β = 0.33, *p value* < 0.001); the interaction between dataset and guild was also significant (β = -0.21, *p value* < 0.001) (Fig. 4b and d).

Functional profiling

Based on the number of assembled transcripts and genes and assembly length, the best assembly was version 1 from Trinity (Table S1). After filtering by expression level, we were able to annotate as “fungi”, with at least one COG assignment, 89,195 (38.5%) of the 231,173 ORFs predicted. Among these ORFs, 57,345 ORFs were observed for needles of both symptomatic and asymptomatic needles, the former presented 16,277 uniquely predicted ORFs, and the latter presented 13,173 ORFs (Fig. 5a). The relative abundance of COG categories was identical between samples from symptomatic and asymptomatic needles (Fig. S3), although 21 of the annotated ORFs exhibited significant expression differences in expression between needle condition (adjusted *p value < 0.05*); twenty of such ORFs were upregulated in the asymptomatic needles, while one was downregulated (Fig. 5b). Six of these ORFs (ORF 4, ORF 11, ORF 16, ORF 5, ORF 7 and ORF 19) have been previously reported in upregulated fungal proteins in response to oxidative stress or redox systems (Table 1).

Table 1
Annotation of significant differentially expressed ORFs

ID	COG category	Preferred name	PFAMs	Description	Stress	Target species
1	S	-	-	-	-	-
2	S	-	Grg1	Pfam:DUF2823	Carbon starvation [96]	*Podospora anserina*
3	G	-	MFS_1	Major facilitator superfamily	Response to toxic compounds [97]	*Colletotrichum higginsianum*
4	GO	-	DUF1996, WSC	Yeast cell wall integrity and stress response	Osmotic, oxidative and cell wall perturbation [83]	*Beauveria bassiana*
5	G	GPD	Gp_dh_C, Gp_dh_N	Glyceraldehyde-3-phosphate dehydrogenase	Salinity [84], Oxidative [85, 86]	*Aspergillus sydowii, Saccharomyces cerevisiae*
6	S	-	But2	Gpi anchored cell wall	-	-
7	S	-	Ferritin_2	Ferritin-like domain	Oxidative [111]	-
8	S	-	CFEM	CFEM domain	Oxidative [91]	*Magnaporthe oryzae*
9	S	-	-	-	-	-
10	E	-	GMC_oxred_C, GMC_oxred_N	Alcohol oxidase	Oxidative [92]	*Aspergillus nidulans*
11	S	-	Peroxidase_2	Peroxidase, family 2	Oxidative [112]	-
12	S	-	GFA	Glutathione-dependent Formaldehyde-activating enzyme	-	-
13	G	-	GFA,SLT	Transglycosylase SLT domain	-	-
14	P	qutD	Sugar_tr	-	-	-
15	Q	-	ADH_N, ADH_N_assoc, ADH_zinc_N	Dehydrogenase	-	-

ID	COG category	Preferred name	PFAMs	Description	Stress	Target species
16	S	-	Peroxidase_2	Peroxidase, family 2	Oxidative [112]	-
17	C	ATP1	ATP-synt_ab, ATP-synt_ab_C, ATP-synt_ab_N	ATP synthase	-	-
18	E	-	DHQ_synthase	3-dehydroquinate synthase	-	-
19	S	-	Ferritin_2	Ferritin-like domain	Oxidative [111]	-
20	G	gel4	Glyco_hydro_72, X8	Beta-glucan production	-	-
21	S	-	Arrestin_C,Arrestin_N	Arrestin (or S-antigen), C-terminal domain	-	-

Discussion

Fungal endophytes from symptomatic and asymptomatic individuals are taxonomically similar

Contrary to our first hypothesis, we did not observe differences in the taxonomic composition of fungal communities of needles from symptomatic and asymptomatic *A. religiosa* needles when using either ITS2 metabarcoding or RNA-seq metatranscriptomics; these included pathogen and endophyte richness and abundance. Classes Dothideomycetes, Eurotiomycetes and Sordariomycetes were the most abundant in our analyses, regardless of the tree condition or dataset used (Fig. 3). These classes are commonly detected in studies characterizing leaf-inhabiting fungal communities of both angiosperms and gymnosperms, e.g., in *Solanum* [67], *Quercus* [68], *Vitis* [69] and *Abies* species such as *A. koreana* [70]. In our study, class Leotiomycetes exhibited a marginally significant increase in observed richness from asymptomatic needles (Fig. 3). This class includes many foliar fungal endophytes that are particularly common in coniferous trees, like *Pinus* and *Abies* [71].

We found only two significantly more abundant OTUs in asymptomatic needles, one identified to belong to genus *Phaeomoniella* and the other belonging to order Lecanorales. *Phaeomoniella* species include the pathogenic *P. chlamydospora*, which has been associated with Petri and esca diseases in grapevines [72], and the epiphytic species *P. zymoides* and *P. pinifoliorum*, which are acidic tolerants [73]. Additional studies are needed to determine the specific role of this genus in *Abies*. In turn, the presence of an OTU belonging to order Lecanorales, a mostly lichenized lineage [74], could represent a propagule of a lichen. Nevertheless, other studies using metabarcoding recorded the presence of some unidentified taxa belonging to this order in leaves of Poaceae and Asteraceae species [75].

Liu et al. [10] reported a shift in the fungal endophyte community of the tree *Euonymus japonicus*, toward a phyllosphere enriched in pathogenic fungi, in plants exposed experimentally to elevated ozone levels (4,500 ~ 11,000 ppb). Although O_3 concentration in the surroundings of Mexico City can reach as high as 117 ppb locally [12], the sampled trees may not have been as exposed as a plant within a greenhouse experiment, where there is no wind that can dissipate air pollutants. Furthermore, other confounding environmental factors, such as drought, may also explain the absence of differences in observed richness or relative abundance of plant pathogens and foliar endophytes between symptomatic and asymptomatic needles.

Interestingly, we found a greater richness and relative abundance of plant pathogens than of foliar endophytes, regardless of needle condition (symptomatic or asymptomatic) (Fig. 4). These differences can be explained by the great diversity of plant pathogens in plant-associated fungal communities [76]. Nevertheless, we must consider that endophytism occurs along a continuum between mutualism and pathogenicity [4]. Thus, it is essential to acknowledge that recognizing a pathogen or an endophytic behavior is not possible with presence data. This is illustrated within the FungalTraits classification [60], where certain OTUs classified as pathogens also exhibit a secondary lifestyle as endophytic fungi (Table S2). Notably, guild assignments (FungalTraits, [60]) require OTU identification at the genus level, which in our case corresponded to only 25.4% (ITS2 metabarcoding) and 45% (for RNA-Seq metatranscriptomics) of the OTUs. This highlights the limited depth of our understanding of the fungal taxa inhabiting *A. religiosa* needles, and of tropical/subtropical endophytic fungal diversity in general [77]. Since eDNA identifications rely on reference databases (i.e., UNITE [35]), our understanding of foliar fungal communities is limited if their identities and functional guilds are uncertain.

Despite the relatively small sample size and unsaturated accumulation curve of our dataset (Fig. S4), other studies with varying sample efforts and plant systems (e.g., *Eucalyptus*, *Vitis* and *Vainilla*) found no differences in fungal endophyte communities between asymptomatic and symptomatic hosts [8, 9, 78]. This could imply that the same taxa can exhibit different behaviors (i.e., as harmless endophytes or pathogens), depending on the strength of the environmental stressor, as has been previously reported for many fungal endophytes [4]. On the other hand, we found a high heterogeneity in the relative abundance of fungal classes across samples (Fig. 3), which may reflect the complexity of factors affecting the assembly of fungal endophyte communities. While environmental conditions, such as O_3, may indirectly influence endophytic microbial communities by affecting plant defense mechanisms [79], its effect over extended periods of time is perhaps relatively less significant that that other biotic and abiotic factors, such as host species, plant genotype or spatial distance [80–82]. For instance, fungal endophyte communities of grapevine are less influenced by pathogen stress than by subtle differences in environmental conditions, such as edaphic composition, temperature, humidity, and sunlight exposure [78].

Fungal endophytes from asymptomatic needles differentially express genes associated with antioxidant mechanisms

As expected in our second hypothesis, we found genes expressed differentially in asymptomatic needles when compared to symptomatic needles (Fig. 5). Eight of the 20 differentially expressed ORFs (ORF 4, ORF 5, ORF 7, ORF 8, ORF 10, ORF 11, ORF 16, and ORF 19) contained domains previously reported in upregulated proteins in response to oxidative stress or redox systems in fungi. For instance, ORF 4 harbors WSC (cell wall stress-responsive component) domains found in the Wsc1I protein, known for its role in detecting stress signals in

Beauveria bassiana [83], including oxidative and osmotic stresses. ORF 5 contains a GPD domain (glycerol-3-phosphate dehydrogenase) that is upregulated in halophilic fungi under high-salinity conditions [84]. This enzyme catalyzes the reduction of NADH to NADPH and the reoxidation to NADH, a cycle associated with the defense of yeast against reactive oxygen species (ROS) during stressful periods [85, 86].

Other overexpressed ORFs related to oxidative stress in asymptomatic needles (ORF 11 and ORF 16) contain a domain of class II peroxidases that catalyze the oxidation of inorganic and organic substrates using H_2O_2 [87]. These peroxidases reduce H_2O_2 and can oxidize a wide range of substrates. Their most prominent association is with lignin decomposition in several white-rot fungi [88], although they are also found in some necrotrophic or hemibiotrophic ascomycetes [89]. Indeed, two Class II peroxidases have been previously found to be upregulated in oxidative stress conditions in the pathogenic fungus *Magnaporthe oryzae* [90]. An additional overexpressed ORF (ORF 8) contains a CFEM domain that has been found in the Pth11 protein that regulates ROS homeostasis during appressorium formation in *Magnaporthe oryzae* [91]. Likewise, ORF 10 contains an alcohol peroxidase domain that is significantly induced in *Aspergillus nidulans* under long-term exposure to oxidative stress [92].

Further upregulated ORFs (ORF 7 and ORF 19) contained ferritin-like domains. Ferritins are recognized in plants and animals for their role in regulating iron levels within cells, and thus preventing ROS formation [93]. While most fungi lack ferritin enzymes [94], some contain ferritin-like sequences in their genomes [95]. It is likely that ferritin-like proteins in fungi play a similar role as those in plants and animals. However, the links between O_3, iron balance, and ferritin-like proteins in fungi remain largely unexplored.

We also detected several upregulated ORFs in needles from asymptomatic needles containing domains associated with other stress responses. For example, ORF 2 (Table 1) has a Grg1 domain whose abundance increases during periods of carbon starvation [96]. Similarly, proteins with the MFS domain, such as ORF 3, play a critical role in transporting both synthetic and naturally occurring toxic compounds [97]. Furthermore, although ORF 20 has not been directly linked to a specific stressor, it contains two domains present in protein gel4, that are relevant for maintaining cell wall integrity in some fungi. Proteins with this domain can also modify cell walls in fungal pathogens, facilitating plant host infection [98].

The only downregulated ORF (ORF 21) found in needles from asymptomatic needles contains two arrestin domains. Arrestins are a family of proteins that play a role in nutrient transport and signaling receptor functions [99]. In fungi, arrestins have been linked to the regulation of several cellular responses. For example, in *Cryptococcus neoformans* arrestins are involved in controlling processes such as cytokinesis, lipid production for cellular membrane formation, and virulence potential [100]. In *Aspergillus nidulans* and *Arthrobotrys oligospora*, arrestins are involved in pH signaling [101, 102]. Furthermore, in *A. oligospora*, arrestins also influence lifestyle changes (from saprotroph to nematophagous), conidial phenotypes, nuclear distribution within cells and stress resistance [102].

RNA-Seq as a tool for mycobiome studies

Our study illustrates that it is possible to use RNA-Seq data available from global sequence repositories to characterize fungal endophyte communities and gene expression, regardless of the plant phenotype. However, since there is no standardized workflow for analyzing fungal sequences, a careful interpretation of the results

and fine-tuned methodologies are needed to address specific questions. The main challenge in using RNA-seq data to characterize endophyte communities lies in the databases available for taxonomic identification using proteins, which often focus on model organisms, neglecting the immense diversity of fungal taxa inhabiting plant tissues. This is crucial because it is difficult to associate potential transcripts with specific taxa.

Other works have used transcripts of the ITS region to identify fungi from RNA-Seq data using ribosomal depletion, which reduces the amount of ribosomal transcripts [103] or by direct amplification of RNA ITS transcripts [104]. However, library construction in our study excluded nonpolyadenylated transcripts, like structural ribosomal RNAs (rRNA) which include the ITS region. Therefore, we did not retrieve sequences from ITS transcripts. The ITS region was selected as the universal fungal barcode [105] and is widely used for the taxonomic identification of fungi using metabarcoding [106]. Therefore, these transcripts would have been very useful for classifying sequences using the available reference databases more accurately (i.e., UNITE [35]). In addition, ITS read numbers would have allowed us to quantify fungal abundances, a task that is currently unreliable using PCR-based methods [107], although care needs to be taken regarding differences in ITS copy numbers among fungal species [108]

Similar to the DNA metabarcoding dataset, we did not find significant differences in the observed richness or relative abundance (Fig. 3) of fungal classes or guilds between symptomatic and asymptomatic needles based on RNA-Seq data. Although the communities recovered using each dataset were different (Fig. 2b), the most representative classes coincided between datasets (Fig. 3). The differences observed could be attributed to the database used to assign taxonomic ranks in each pipeline. For instance, when we examined fungal classes exclusive to the RNA-Seq metatranscriptomics dataset, we found that they comprised predominantly model taxa, such as *Saccharomyces* or *Aspergillus*, indicating a potential bias in classification (Table S2). This bias could be reduced by implementing a database that integrates information on environmental taxa, similar to the JGI Mycocosm database [109], which was previously used in metatranscriptomic studies of plant-associated fungi [110]. The two datasets further differed in the greater observed richness and relative abundance of both foliar endophytes and plant pathogens in the RNA-Seq dataset (Fig. 3, which was accompanied by a narrower variance in this dataset.

Conclusions

Tropospheric ozone affects plants at several levels, including their associated mycobiome. We characterized the endophytic fungal community in symptomatic and asymptomatic needles of *A. religiosa* from a peripheral forest next to Mexico City that has been heavily exposed to O_3 contamination for over 40 years [12]. Our results reveal an intriguing pattern: while symptomatic and asymptomatic needles harbor similar fungal communities, they exhibit varying responses depending on the presence of O_3-related symptoms in their hosts. Notably, our observations indicate that genes associated with oxidative stress response are upregulated in fungi from asymptomatic needles, which suggests that endophytic fungi respond to the oxidative stress triggered by O_3. Moreover, we observed the regulation of other metabolic pathways, such as iron homeostasis, cell integrity maintenance, and detoxification of toxic compounds, which indicated that these mechanisms collectively enhanced the performance of fungal communities within asymptomatic needles, benefiting the host plant. However, further studies are needed to demonstrate that fungal endophytes may affect and even enhance the host performance when O_3 concentrations increase, including controlled experiments where the effects of

other cooccurring pollutants can be discarded. Future research exploring cotranscription networks between host and fungal communities could help infer such correlations between host plant and fungal endophyte responses to O_3 stress. Finally, we demonstrated that it is possible to use plant RNA-seq metatranscriptomics to gain broad insight into plant-inhabiting fungi and their response to stress; such approaches have limitations that should be addressed in future studies.

Declarations

Acknowledgments

This paper is part of the requirements of VSFA for obtaining a M.Sc. degree with a specialization in the field of ecology at Posgrado en Ciencias Biológicas, UNAM. Computational analyses were performed using the High Performance Cluster of CONABIO and Centro de Ciencias Genómicas, UNAM. We thank Luis Alfredo Hernández-Hernández for his assistance in preparing the distribution map of *Abies religiosa* in Mexico, Leonardo Peraza-Reyes for his comments to improve the manuscript and Jeff Stallman for his review of the English language in this manuscript.

Funding

Financing was granted by FORDECYT 2019-5 Project 308488, PRONACES Sistemas Socioecológicos 2021 Project 319083 and a CONAHCYT graduate scholarship to VSFA.

Author information

Authors and affiliations

Posgrado en Ciencias Biológicas, Universidad Nacional Autónoma de México, Av. Ciudad Universitaria 3000, Z.C. 04510, Coyoacán, Ciudad de México, Mexico

Valeria Stephany Flores-Almaraz

ORCID: 0009-0003-8601-8462

Instituto de Biología, Universidad Nacional Autónoma de México, Av. Ciudad Universitaria 3000, 04510, Coyoacán, Ciudad de México, Mexico

Valeria Stephany Flores-Almaraz

Royal Botanic Gardens Victoria, Birdwood Ave, Melbourne, VIC 3004, Australia

Camille Truong

ORCID: 0000-0002-8510-1761

Centro de Ciencias Genómicas, Universidad Nacional Autónoma de México, Av. Universidad S/N, 62210. Cuernavaca, Morelos, México

Diana Hernández-Oaxaca

ORCID: 0000-0001-6218-8297

Depto. de Ecología Evolutiva, Instituto de Ecología, Universidad Nacional Autónoma de México, Av. Ciudad Universitaria 3000, 04510, Coyoacán, Ciudad de México, Mexico

Juan Pablo Jaramillo Correa

ORCID: 0000-0001-7617-913X

Verónica Reyes-Galindo

ORCID: 0000-0003-0688-2203

Consejo Nacional de Humanidades Ciencias y Tecnología (CONAHCYT), Avenida Insurgentes Sur 1582, Crédito Constructor, Benito Juárez, Ciudad de México. C.P. 03940. México.

Alicia Mastretta-Yanes

ORCID: 0000-0003-2951-6353

Comisión Nacional para el Conocimiento y Uso de la Biodiversidad (CONABIO). Avenida Liga Periférico-Insurgentes Sur 4903. Colonia Parques del Pedregal, Tlalpan, Ciudad de México. CP 14010. México

Alicia Mastretta-Yanes

Laboratorios de Micología. Depto. de Biología Comparada, Facultad de Ciencias. Universidad Nacional Autónoma de México, Circuito Exterior s/n, Ciudad Universitaria, Coyoacán, 04510. Ciudad de México, México

Rodolfo Salas-Lizana

Contributions

VSFA, CT, AMY, JPJC, and RSL conceived and designed the analysis; CT and VRG collected and acquired the data, VSFA and DHO performed the bioinformatics analyses; and VSFA, CT, and RSL wrote the paper. All the authors contributed to the data interpretation, drafting, and revision of the manuscript.

Corresponding author

Rodolfo Salas-Lizana

Ethics declarations

Consent to participate

All the authors consented to participate in this publication during the drafting phase and contributed to the revision of the manuscript.

Consent for Publication

All the authors consent to the publication of this research.

Conflict of Interest

The authors declare no conflict of interest.

Competing Interests

The authors declare no competing interests.

References

1. Agathokleous E, Feng Z, Oksanen E et al (2020) Ozone affects plant, insect, and soil microbial communities: A threat to terrestrial ecosystems and biodiversity. Sci Adv 6. https://doi.org/10.1126/sciadv.abc1176
2. Grulke NE, Heath RL (2020) Ozone effects on plants in natural ecosystems. Plant Biol 22:12–37. https://doi.org/10.1111/plb.12971
3. Stone JK, Bacon CW, White JF (2000) An Overview of Endophytic Microbes. Endophytism Defined
4. Schulz B, Boyle C (2005) The endophytic continuum. Mycol Res 109:661–686. https://doi.org/10.1017/S095375620500273X
5. Rodriguez RJ, White JF, Arnold AE, Redman RS (2009) Fungal endophytes: Diversity and functional roles: Tansley review. New Phytol 182:314–330. https://doi.org/10.1111/j.1469-8137.2009.02773.x
6. Hereme R, Morales-Navarro S, Ballesteros G et al (2020) Fungal Endophytes Exert Positive Effects on Colobanthus quitensis Under Water Stress but Neutral Under a Projected Climate Change Scenario in Antarctica. Front Microbiol 11. https://doi.org/10.3389/fmicb.2020.00264
7. Wemheuer F, Wemheuer B, Daniel R, Vidal S (2019) Deciphering bacterial and fungal endophyte communities in leaves of two maple trees with green islands. Sci Rep 9:14183. https://doi.org/10.1038/s41598-019-50540-2
8. Messal M, Slippers B, Naidoo S et al (2019) Active Fungal Communities in Asymptomatic Eucalyptus grandis Stems Differ between a Susceptible and Resistant Clone. Microorganisms 7:375. https://doi.org/10.3390/microorganisms7100375
9. Carbajal-Valenzuela IA, Muñoz-Sanchez AH, Hernández-Hernández J et al (2022) Microbial Diversity in Cultivated and Feral Vanilla Vanilla planifolia Orchids Affected by Stem and Rot Disease. Microb Ecol 84:821–833. https://doi.org/10.1007/s00248-021-01876-8
10. Liu J, Song M, Wei X et al (2022) Responses of phyllosphere microbiome to ozone stress: abundance, community compositions and functions. Microorganisms 10. https://doi.org/10.3390/microorganisms10040680
11. Javed J, Rauf M, Arif M et al (2022) Endophytic Fungal Consortia Enhance Basal Drought-Tolerance in Moringa oleifera by Upregulating the Antioxidant Enzyme (APX) through Heat Shock Factors. Antioxidants 11:1669. https://doi.org/10.3390/antiox11091669

12. SEDEMA (2020) Calidad del Aire en la Ciudad de México. Informe Anual
13. De Bauer M, de de L, Hernández-Tejeda T (2007) A review of ozone-induced effects on the forests of central Mexico. Environ Pollut 147:446–453. https://doi.org/10.1016/j.envpol.2006.12.020
14. Reyes-Galindo V, Jaramillo-Correa JP, Nava KC et al (2023) Evaluating pollution-related damage and restoration success in urban forests with participatory monitoring and digital tools. Conserv Biol. https://doi.org/10.1111/cobi.14112
15. Mills G, Pleijel H, Büker P et al (2010) Chap. 3: mapping critical levels for vegetation. Mapping manual. Manual on methodologies and criteria for modelling and mapping critical loads and levels; and air pollution effects, risks and trends
16. Alvarez D, Laguna G, Rosas I (1998) Macroscopic and microscopic symptoms in Abies religiosa exposed to ozone in a forest near Mexico City. Environ Pollut 103:251–259. https://doi.org/10.1016/S0269-7491(98)00113-4
17. Martínez-Méndez N, Aguirre-Planter E, Eguiarte LE, Jaramillo-Correa JP (2016) Modelado de nicho ecológico de las especies del género Abies (Pinaceae) en México: Algunas implicaciones taxonómicas y para la conservación. Bot Sci 94:5–24. https://doi.org/10.17129/botsci.508
18. INEGI (2015) Delimitación de las zonas metropolitanas de México 2015
19. Rzedowski J (2006) Vegetación de México. Comisión Nacional para el Conocimiento y Uso de la Biodiversidad, México
20. Hernández-Álvarez AG, Reyes-Ortiz JL, Villanueva-Díaz J, Sánchez-González A (2021) Variación en la estructura del bosque de Abies religiosa (Pinaceae), en diferentes condiciones de manejo y disturbio. Acta Bot Mex. https://doi.org/10.21829/abm128.2021.1752
21. CONANP (2006) Programa de Conservacion y Manejo. Parque Nacional Desierto de los Leones
22. Hernández-Tejeda T, Benavides-Meza HM (2018) Sensibilidad de 20 procedencias de pino y oyamel a los oxidantes fotoquímicos. Rev Mex Cienc For 6:32–51. https://doi.org/10.29298/rmcf.v6i30.206
23. Reyes-Galindo V (2019) Análisis transcriptómico de la tolerancia a ozono troposférico en Abies religiosa
24. Bandurska H, Borowiak K, Zielezińska M (2023) Oxidative stress enzymes in tobacco during a long-term exposure to ambient ozone at two different sites. Arch Environ Prot. https://doi.org/10.24425/aep.2018.122297
25. Savi GD, Scussel VM (2014) Effects of Ozone Gas Exposure on Toxigenic Fungi Species from Fusarium, Aspergillus, and Penicillium Genera. Ozone Sci Eng 36:144–152. https://doi.org/10.1080/01919512.2013.846824
26. Ali EM, Abdallah BM (2022) The potential use of ozone as antifungal and antiaflatoxigenic agent in nuts and its effect on nutritional quality. Braz J Biol 84:e263814. https://doi.org/10.1590/1519-6984.263814
27. Gonzalez E, Pitre FE, Pagé AP et al (2018) Trees, fungi and bacteria: tripartite metatranscriptomics of a root microbiome responding to soil contamination. Microbiome 6:53. https://doi.org/10.1186/s40168-018-0432-5
28. Zhang J, Wang X, Wang H-T et al (2023) Overexpression of REDUCED WALL ACETYLATION C increases xylan acetylation and biomass recalcitrance in Populus. Plant Physiol kiad377. https://doi.org/10.1093/plphys/kiad377

29. Lim PK, Zheng X, Goh JC, Mutwil M (2022) Exploiting plant transcriptomic databases: Resources, tools, and approaches. Plant Commun 3:100323. https://doi.org/10.1016/j.xplc.2022.100323
30. Chialva M, Ghignone S, Novero M et al (2019) Tomato RNA-seq Data Mining Reveals the Taxonomic and Functional Diversity of Root-Associated Microbiota. Microorganisms 8:38. https://doi.org/10.3390/microorganisms8010038
31. Alvarado-Rosales D, Hernández-Tejeda T (2002) Decline of Sacred Fir in the Desierto de los Leones National Park. In: Fenn ME, De Bauer LI, Hernández-Tejeda T (eds) Urban Air Pollution and Forests. Springer New York, New York, NY, pp 243–260
32. Tedersoo L, Lindahl B (2016) Fungal identification biases in microbiome projects. Environ Microbiol Rep 8:774–779. https://doi.org/10.1111/1758-2229.12438
33. Palmer JM, Jusino MA, Banik MT, Lindner DL (2018) Non-biological synthetic spike-in controls and the AMPtk software pipeline improve mycobiome data. PeerJ 6:e4925. https://doi.org/10.7717/peerj.4925
34. Bermúdez-Contreras AI, Monroy-Guzmán C, Pérez-Lucas L et al (2022) Mycorrhizal Fungi Associated With Juniper and Oak Seedlings Along a Disturbance Gradient in Central Mexico. Front For Glob Change. https://doi.org/10.3389/ffgc.2022.736664. 5:
35. Nilsson RH, Larsson K-H, Taylor AFS et al (2019) The UNITE database for molecular identification of fungi: handling dark taxa and parallel taxonomic classifications. Nucleic Acids Res 47:D259–D264. https://doi.org/10.1093/nar/gky1022
36. Nguyen NH, Smith D, Peay K, Kennedy P (2015) Parsing ecological signal from noise in next generation amplicon sequencing. New Phytol 205:1389–1393. https://doi.org/10.1111/nph.12923
37. Truong C, Gabbarini LA, Corrales A et al (2019) Ectomycorrhizal fungi and soil enzymes exhibit contrasting patterns along elevation gradients in southern Patagonia. New Phytol 222:1936–1950. https://doi.org/10.1111/nph.15714
38. Bolger AM, Lohse M, Usadel B (2014) Trimmomatic: a flexible trimmer for Illumina sequence data. Bioinformatics 30:2114–2120. https://doi.org/10.1093/bioinformatics/btu170
39. Andrews S (2010) FastQC: a quality control tool for high throughput sequence data
40. Ewels P, Magnusson M, Lundin S, Käller M (2016) MultiQC: summarize analysis results for multiple tools and samples in a single report. Bioinformatics 32:3047–3048. https://doi.org/10.1093/bioinformatics/btw354
41. Li H (2013) Aligning sequence reads, clone. sequences and assembly contigs with BWA-MEM
42. Bankevich A, Nurk S, Antipov D et al (2012) SPAdes: A New Genome Assembly Algorithm and Its Applications to Single-Cell Sequencing. J Comput Biol 19:455–477. https://doi.org/10.1089/cmb.2012.0021
43. Gurevich A, Saveliev V, Vyahhi N, Tesler G (2013) QUAST: quality assessment tool for genome assemblies. Bioinformatics 29:1072–1075. https://doi.org/10.1093/bioinformatics/btt086
44. Grabherr MG, Haas BJ, Yassour M et al (2011) Full-length transcriptome assembly from RNA-Seq data without a reference genome. Nat Biotechnol 29:644–652. https://doi.org/10.1038/nbt.1883
45. Li B, Dewey CN (2011) RSEM: accurate transcript quantification from RNA-Seq data with or without a reference genome. BMC Bioinformatics 12:323. https://doi.org/10.1186/1471-2105-12-323

46. Mikheenko A, Saveliev V, Gurevich A (2016) MetaQUAST: evaluation of metagenome assemblies. Bioinformatics 32:1088–1090. https://doi.org/10.1093/bioinformatics/btv697
47. Wood DE, Lu J, Langmead B (2019) Improved metagenomic analysis with Kraken 2. Genome Biol 20:257. https://doi.org/10.1186/s13059-019-1891-0
48. Lu J, Breitwieser FP, Thielen P, Salzberg SL (2017) Bracken: estimating species abundance in metagenomics data. PeerJ Comput Sci 3:e104. https://doi.org/10.7717/peerj-cs.104
49. Menzel P, Ng KL, Krogh A (2016) Fast and sensitive taxonomic classification for metagenomics with Kaiju. Nat Commun 7:11257. https://doi.org/10.1038/ncomms11257
50. R Core Team (2021) R: A language and environment for statistical and computing
51. McMurdie PJ, Holmes S (2013) phyloseq: An R Package for Reproducible Interactive Analysis and Graphics of Microbiome Census Data. PLoS ONE 8:e61217. https://doi.org/10.1371/journal.pone.0061217
52. Yan L (2021) Draw Venn Diagram by ggplot2 [R package ggvenn version 0.1.9]
53. Lahti L, Shetty S et al (2019) Tools for microbiome analysis in R. Microbiome package
54. Oksanen J, Kindt R, Legendre P et al (2008) vegan: Community Ecology Package
55. Larsson J (2022) eulerr: Area-Proportional Euler and Venn Diagrams with Ellipses
56. Wickham H (2016) ggplot2: Elegant Graphics for Data Analysis. Springer-Verlag
57. Love MI, Huber W, Anders S (2014) Moderated estimation of fold change and dispersion for RNA-seq data with DESeq2. Genome Biol 15:550. https://doi.org/10.1186/s13059-014-0550-8
58. Cáceres MD, Legendre P (2009) Associations between species and groups of sites: indices and statistical inference. Ecology 90:3566–3574. https://doi.org/10.1890/08-1823.1
59. Andersen KS, Kirkegaard RH, Karst SM, Albertsen M (2018) ampvis2: an R package to analyse and visualise 16S rRNA amplicon data. bioRxiv. https://doi.org/10.1101/299537
60. Põlme S, Abarenkov K, Henrik Nilsson R et al (2020) FungalTraits: a user-friendly traits database of fungi and fungus-like stramenopiles. Fungal Divers 105:1–16. https://doi.org/10.1007/s13225-020-00466-2
61. Dufrêne M, Legendre P SPECIES ASSEMBLAGES AND INDICATOR, SPECIES:THE NEED, FOR A FLEXIBLE ASYMMETRICAL APPROACH (1997). Ecol Monogr 67:345–366. https://doi.org/10.1890/0012-9615(1997)067[0345:SAAIST]2.0.CO;2
62. Hass B (in prep) Transdecoder
63. Cantalapiedra CP, Hernández-Plaza A, Letunic I et al (2021) eggNOG-mapper v2: Functional Annotation, Orthology Assignments, and Domain Prediction at the Metagenomic Scale. Mol Biol Evol 38:5825–5829. https://doi.org/10.1093/molbev/msab293
64. Huerta-Cepas J, Szklarczyk D, Heller D et al (2019) eggNOG 5.0: a hierarchical, functionally and phylogenetically annotated orthology resource based on 5090 organisms and 2502 viruses. Nucleic Acids Res 47:D309–D314. https://doi.org/10.1093/nar/gky1085
65. Patro R, Duggal G, Love MI et al (2017) Salmon provides fast and bias-aware quantification of transcript expression. Nat Methods 14:417–419. https://doi.org/10.1038/nmeth.4197
66. Soneson C, Love MI, Robinson MD (2016) Differential analyses for RNA-seq: transcript-level estimates improve gene-level inferences. F1000Research 4:1521. https://doi.org/10.12688/f1000research.7563.2

67. Dong C, Wang L, Li Q, Shang Q (2021) Epiphytic and Endophytic Fungal Communities of Tomato Plants. Hortic Plant J 7:38–48. https://doi.org/10.1016/j.hpj.2020.09.002
68. Nguyen MH, Shin KC, Lee JK (2021) Fungal Community Analyses of Endophytic Fungi from Two Oak Species, Quercus mongolica and Quercus serrata, in Korea. Mycobiology 49:385–395. https://doi.org/10.1080/12298093.2021.1948175
69. Aleynova OA, Nityagovsky NN, Suprun AR et al (2022) The Diversity of Fungal Endophytes from Wild Grape Vitis amurensis Rupr. Plants 11:2897. https://doi.org/10.3390/plants11212897
70. Choi BY, Lee S, Kim J et al (2022) Comparison of Endophytic and Epiphytic Microbial Communities in Surviving and Dead Korean Fir (Abies koreana) Using Metagenomic Sequencing. Forests 13:1932. https://doi.org/10.3390/f13111932
71. Arnold AE (2007) Understanding the diversity of foliar endophytic fungi: progress, challenges, and frontiers. Fungal Biol Rev 21:51–66. https://doi.org/10.1016/j.fbr.2007.05.003
72. Crous PW, Gams W (2000) Phaeomoniella chlamydospora gen. et comb. nov., a causal organism of Petri grapevine decline and esca. Phytopathol Mediterr 39:112–118
73. Lee HB, Park JY, Jung HS, Summerbell RC (2006) Phaeomoniella zymoides and Phaeomoniella pinifoliorum spp. nov., new acid-tolerant epiphytic fungi isolated from pine needles in Korea. Mycologia 98:598–611. https://doi.org/10.1080/15572536.2006.11832663
74. Honegger R (2012) 15 The Symbiotic Phenotype of Lichen-Forming Ascomycetes and Their Endo- and Epibionts. In: Hock B (ed) Fungal Associations. Springer Berlin Heidelberg, Berlin, Heidelberg, pp 287–339
75. Ricks KD, Koide RT (2019) The role of inoculum dispersal and plant species identity in the assembly of leaf endophytic fungal communities. PLoS ONE 14:e0219832. https://doi.org/10.1371/journal.pone.0219832
76. Tanunchai B, Ji L, Schroeter SA et al (2023) FungalTraits vs. FUNGuild: Comparison of Ecological Functional Assignments of Leaf- and Needle-Associated Fungi Across 12 Temperate Tree Species. Microb Ecol 85:411–428. https://doi.org/10.1007/s00248-022-01973-2
77. Narvaez-Trujillo A, Marchán-Rivadeneira MR, Veloz-Villavicencio E, Portero CE (2021) What Do We Know About Fungal Endophyte Diversity in a Mega Diverse Country? An Appeal for Increased Conservation and Research. In: Rosa LH (ed) Neotropical Endophytic Fungi. Springer International Publishing, Cham, pp 131–149
78. Geiger A, Karácsony Z, Golen R et al (2022) The Compositional Turnover of Grapevine-Associated Plant Pathogenic Fungal Communities Is Greater Among Intraindividual Microhabitats and Terroirs than Among Healthy and Esca-Diseased Plants. Phytopathology® 112:1029–1035. https://doi.org/10.1094/PHYTO-05-21-0190-R
79. Agler MT, Ruhe J, Kroll S et al (2016) Microbial Hub Taxa Link Host and Abiotic Factors to Plant Microbiome Variation. PLOS Biol 14:e1002352. https://doi.org/10.1371/journal.pbio.1002352
80. Zuo Y, Li X, Yang J et al (2021) Fungal Endophytic Community and Diversity Associated with Desert Shrubs Driven by Plant Identity and Organ Differentiation in Extremely Arid Desert Ecosystem. J Fungi 7:578. https://doi.org/10.3390/jof7070578
81. Bell-Dereske LP, Evans SE (2021) Contributions of environmental and maternal transmission to the assembly of leaf fungal endophyte communities. Proc R Soc B Biol Sci 288:20210621.

https://doi.org/10.1098/rspb.2021.0621

82. Harris MA, Kemler M, Slippers B et al (2023) Deterministic processes have limited impacts on foliar fungal endophyte communities along a savanna-forest successional gradient. Fungal Ecol 64:101249. https://doi.org/10.1016/j.funeco.2023.101249
83. Tong S, Wang D, Gao B et al (2019) The DUF1996 and WSC domain-containing protein Wsc1I acts as a novel sensor of multiple stress cues in Beauveria bassiana. Cell Microbiol 21. https://doi.org/10.1111/cmi.13100
84. Pérez-Llano Y, Rodríguez-Pupo EC, Druzhinina IS et al (2020) Stress Reshapes the Physiological Response of Halophile Fungi to Salinity. Cells 9:525. https://doi.org/10.3390/cells9030525
85. Ansell R, Granath K, Hohmann S et al (1997) The two isoenzymes for yeast NAD $^{+}$ -dependent glycerol 3-phosphate dehydrogenase encoded by GPD1 and GPD2 have distinct roles in osmoadaptation and redox regulation. EMBO J 16:2179–2187. https://doi.org/10.1093/emboj/16.9.2179
86. Hohmann S (2002) Osmotic Stress Signaling and Osmoadaptation in Yeasts. Microbiol Mol Biol Rev 66:300–372. https://doi.org/10.1128/MMBR.66.2.300-372.2002
87. Conesa A, Punt PJ, Van Den Hondel CAMJJ (2002) Fungal peroxidases: molecular aspects and applications. J Biotechnol 93:143–158. https://doi.org/10.1016/S0168-1656(01)00394-7
88. Lundell TK, Mäkelä MR, Hildén K (2010) Lignin-modifying enzymes in filamentous basidiomycetes - ecological, functional and phylogenetic review: Lignin-modifying enzymes in filamentous basidiomycetes - ecological, functional and phylogenetic review. J Basic Microbiol 50:5–20. https://doi.org/10.1002/jobm.200900338
89. Ballesteros GI, Torres-Díaz C, Bravo LA et al (2020) In silico analysis of metatranscriptomic data from the Antarctic vascular plant Colobanthus quitensis: Responses to a global warming scenario through changes in fungal gene expression levels. Fungal Ecol 43. https://doi.org/10.1016/j.funeco.2019.100873
90. Mir AA, Park S-Y, Sadat MA et al (2015) Systematic characterization of the peroxidase gene family provides new insights into fungal pathogenicity in Magnaporthe oryzae. Sci Rep 5:11831. https://doi.org/10.1038/srep11831
91. Kou Y, Tan YH, Ramanujam R, Naqvi NI (2017) Structure–function analyses of the Pth11 receptor reveal an important role for CFEM motif and redox regulation in rice blast. New Phytol 214:330–342. https://doi.org/10.1111/nph.14347
92. Pusztahelyi T, Klement É, Szajli E et al (2011) Comparison of transcriptional and translational changes caused by long-term menadione exposure in Aspergillus nidulans. Fungal Genet Biol 48:92–103. https://doi.org/10.1016/j.fgb.2010.08.006
93. Orino K, Lehman L, Tsuji Y et al (2001) Ferritin and the response to oxidative stress. Biochem J 357:241–247. https://doi.org/10.1042/bj3570241
94. Schrettl M, Haas H (2011) Iron homeostasis—Achilles' heel of Aspergillus fumigatus? Curr Opin Microbiol 14:400–405. https://doi.org/10.1016/j.mib.2011.06.002
95. Canessa P, Larrondo LF (2013) Environmental responses and the control of iron homeostasis in fungal systems. Appl Microbiol Biotechnol 97:939–955. https://doi.org/10.1007/s00253-012-4615-x

96. Kimpel E, Osiewacz HD (1999) PaGrg1, a glucose-repressible gene of Podospora anserina that is differentially expressed during lifespan. Curr Genet 35:557–563. https://doi.org/10.1007/s002940050453
97. Liu L, Yan Y, Huang J et al (2017) A Novel MFS Transporter Gene ChMfs1 Is Important for Hyphal Morphology, Conidiation, and Pathogenicity in Colletotrichum higginsianum. Front Microbiol 8:1953. https://doi.org/10.3389/fmicb.2017.01953
98. Samalova M, Mélida H, Vilaplana F et al (2017) The β-1,3-glucanosyltransferases (Gels) affect the structure of the rice blast fungal cell wall during appressorium-mediated plant infection. Cell Microbiol 19. https://doi.org/10.1111/cmi.12659
99. Gurevich EV, Gurevich VV (2006) Arrestins: ubiquitous regulators of cellular signaling pathways. Genome Biol 7:236. https://doi.org/10.1186/gb-2006-7-9-236
100. Telzrow CL, Nichols CB, Castro-Lopez N et al (2019) A Fungal Arrestin Protein Contributes to Cell Cycle Progression and Pathogenesis. mBio 10:e02682–e02619. https://doi.org/10.1128/mBio.02682-19
101. Herranz S, Rodríguez JM, Bussink H-J et al (2005) Arrestin-related proteins mediate pH signaling in fungi. Proc Natl Acad Sci 102:12141–12146. https://doi.org/10.1073/pnas.0504776102
102. Zhou L, Li M, Cui P et al (2022) Arrestin-Coding Genes Regulate Endocytosis, Sporulation, Pathogenicity, and Stress Resistance in Arthrobotrys oligospora. Front Cell Infect Microbiol 12. https://doi.org/10.3389/fcimb.2022.754333
103. Li F, Hitch TCA, Chen Y et al (2019) Comparative metagenomic and metatranscriptomic analyses reveal the breed effect on the rumen microbiome and its associations with feed efficiency in beef cattle. Microbiome 7:6. https://doi.org/10.1186/s40168-019-0618-5
104. Guerreiro MA, Kambach S, Stoll R et al (2023) Linking processes to community functions—insights into litter decomposition combining fungal metatranscriptomics and environmental NMR profiling. Mycol Prog 22:10. https://doi.org/10.1007/s11557-022-01859-0
105. Schoch CL, Robbertse B, Robert V et al (2014) Finding needles in haystacks: linking scientific names, reference specimens and molecular data for Fungi. Database 2014:bau061–bau061. https://doi.org/10.1093/database/bau061
106. Tedersoo L, Bahram M, Zinger L et al (2022) Best practices in metabarcoding of fungi: From experimental design to results. Mol Ecol 31:2769–2795. https://doi.org/10.1111/mec.16460
107. Marcelino VR, Irinyi L, Eden J-S et al (2019) Metatranscriptomics as a tool to identify fungal species and subspecies in mixed communities – a proof of concept under laboratory conditions. IMA Fungus 10:12. https://doi.org/10.1186/s43008-019-0012-8
108. Bradshaw MJ, Aime MC, Rokas A et al (2023) Extensive intragenomic variation in the internal transcribed spacer region of fungi. iScience 26:107317. https://doi.org/10.1016/j.isci.2023.107317
109. Ahrendt SR, Mondo SJ, Haridas S, Grigoriev IV (2023) MycoCosm, the JGI's Fungal Genome Portal for Comparative Genomic and Multiomics Data Analyses. In: Martin F, Uroz S (eds) Microbial Environmental Genomics (MEG). Springer US, New York, NY, pp 271–291
110. Schneider AN, Sundh J, Sundström G et al (2021) Comparative Fungal Community Analyses Using Metatranscriptomics and Internal Transcribed Spacer Amplicon Sequencing from Norway Spruce. mSystems 6:e00884–e00820. https://doi.org/10.1128/mSystems.00884-20

111. Brandon M, Howard B, Lawrence C, Laubenbacher R (2015) Iron acquisition and oxidative stress response in aspergillus fumigatus. BMC Syst Biol 9:19. https://doi.org/10.1186/s12918-015-0163-1

112. Lee Y, Son H, Shin JY et al (2018) Genome-wide functional characterization of putative peroxidases in the head blight fungus Fusarium graminearum: Roles of peroxidases in Fusarium graminearum. Mol Plant Pathol 19:715–730. https://doi.org/10.1111/mpp.12557

113. NCBI (2022) COG [Internet]. COG Internet

Figures

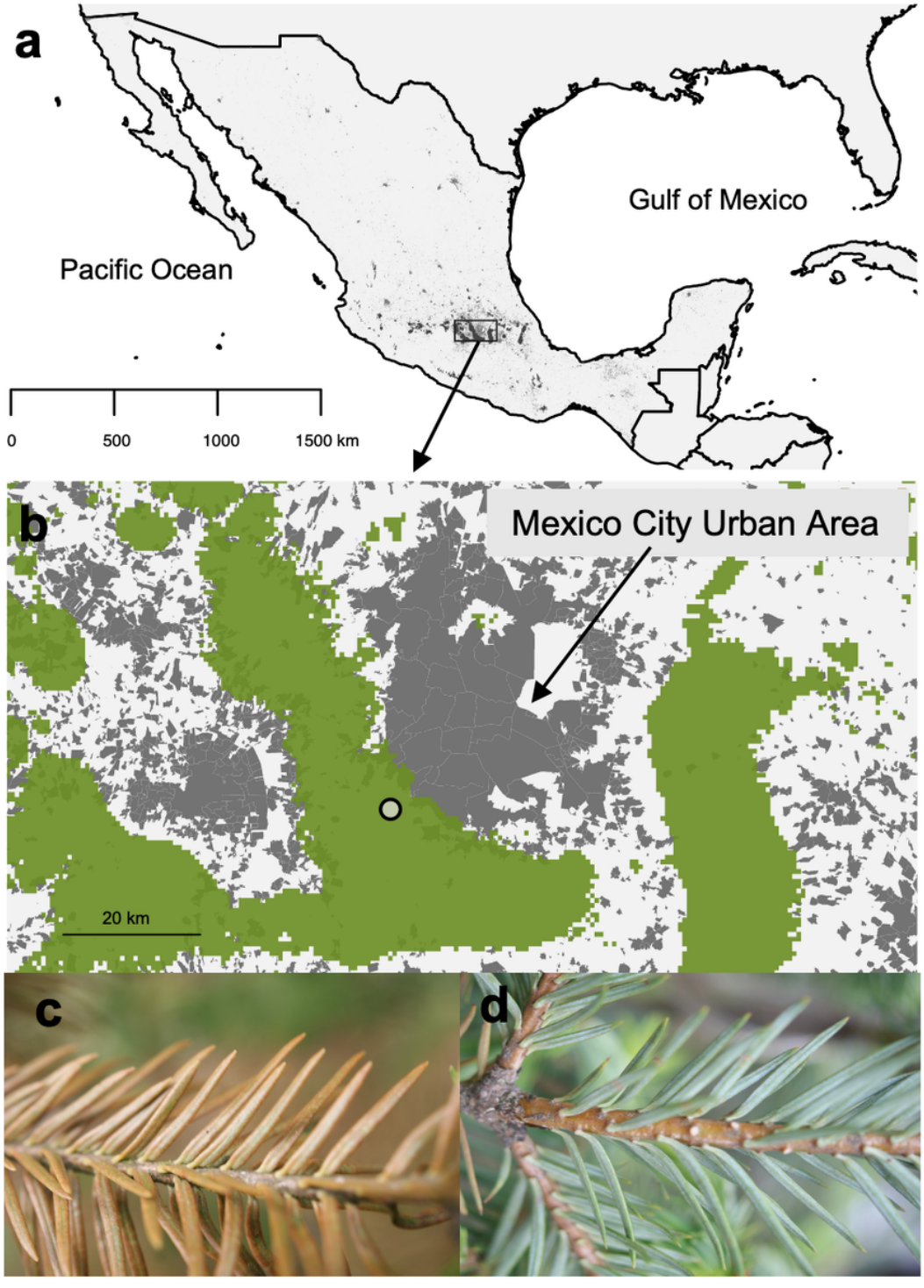

Figure 1

a Distribution of *Abies religiosa* in Mexico; **b** Approximate distribution of the species (green areas; taken from [17]) and neighboring urban and rural zones (gray areas; according to INEGI [18]) in central Mexico. The circle in the forest area depicts the approximate location of the area of study; **c** symptomatic needles. Note the reddish tones toward the base of the branch; and **d**, asymptomatic needles

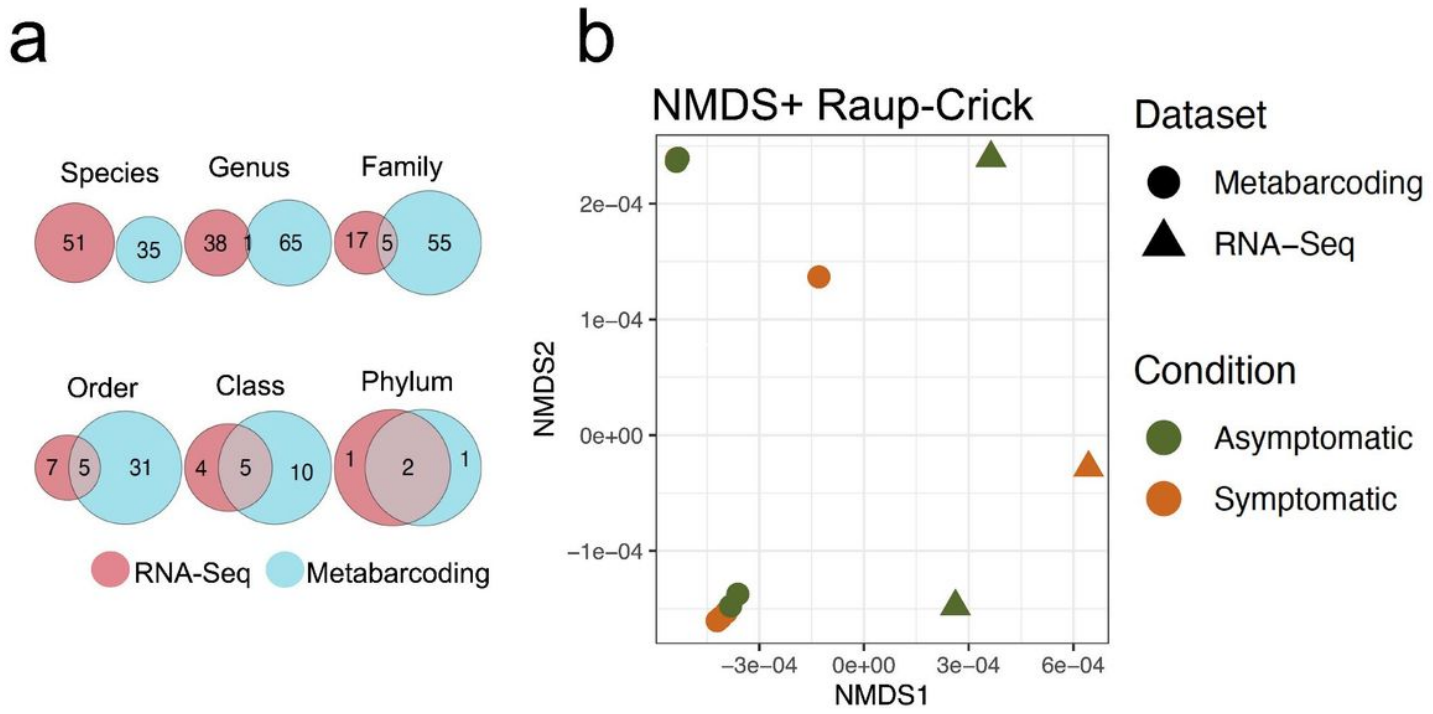

Figure 2

Taxonomic characterization of the fungal endophyte community of needles from symptomatic and asymptomatic *Abies religiosa* individuals (condition) using ITS2 metabarcoding and RNA-seq metatranscriptomics (dataset). **a** Venn diagrams showing the number of shared classified taxa between datasets at each taxonomic level**. b** Nonmetric multidimensional scaling (NMDS) based on Raup–Crick distances showing significant differences in fungal community composition between datasets (PERMANOVA: R^2=1, *p value*= 0.001) but not between conditions

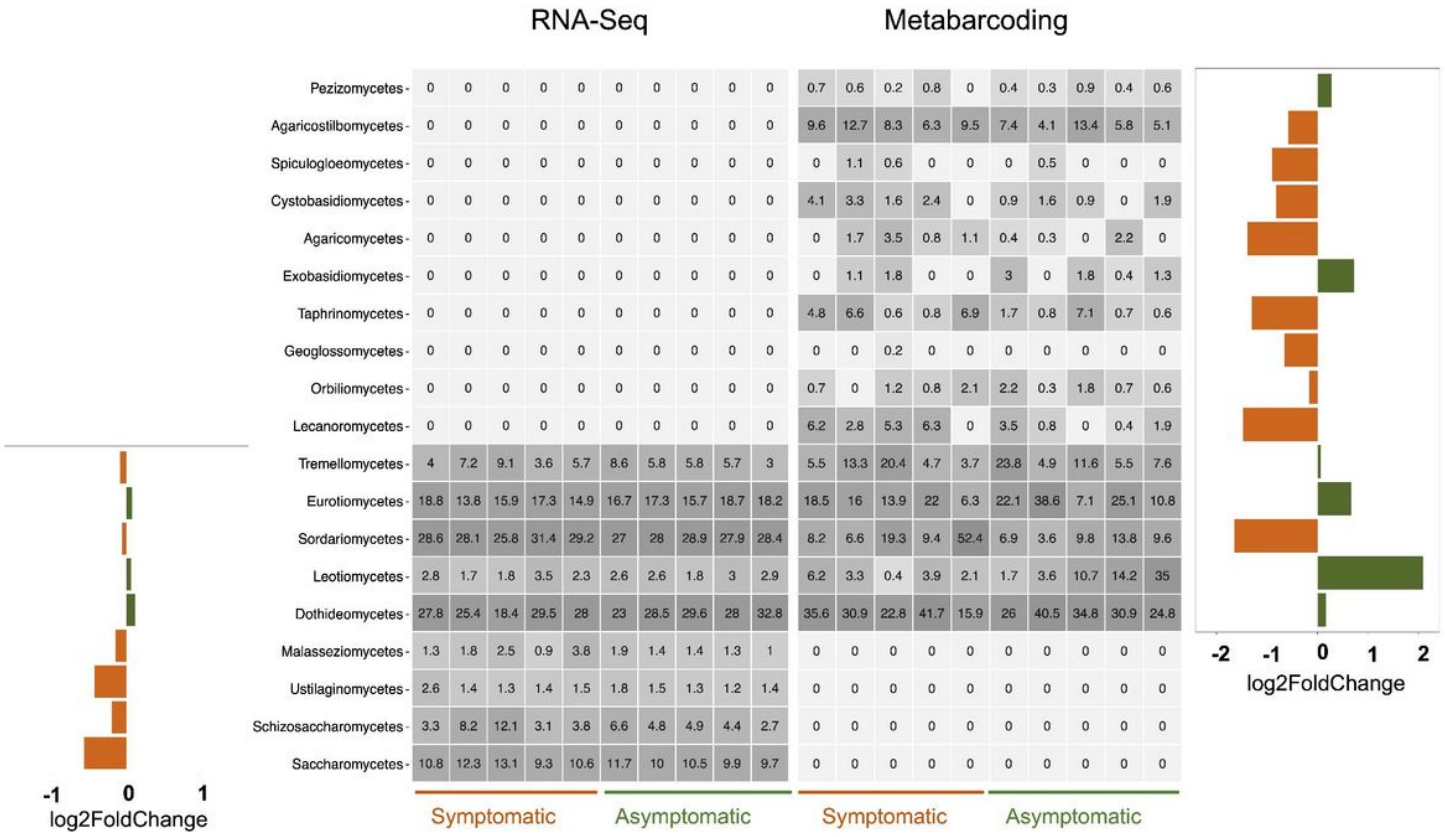

Figure 3

Taxonomic abundance of fungal classes within the endophyte community from symptomatic and asymptomatic needles determined via ITS2 metabarcoding and RNA-seq metatranscriptomics. Heatmap depicts the relative abundance of each identified fungal class per sample. Bar plots show differences in relative abundance changes (represented as log_2FoldChange) between symptomatic and asymptomatic needles

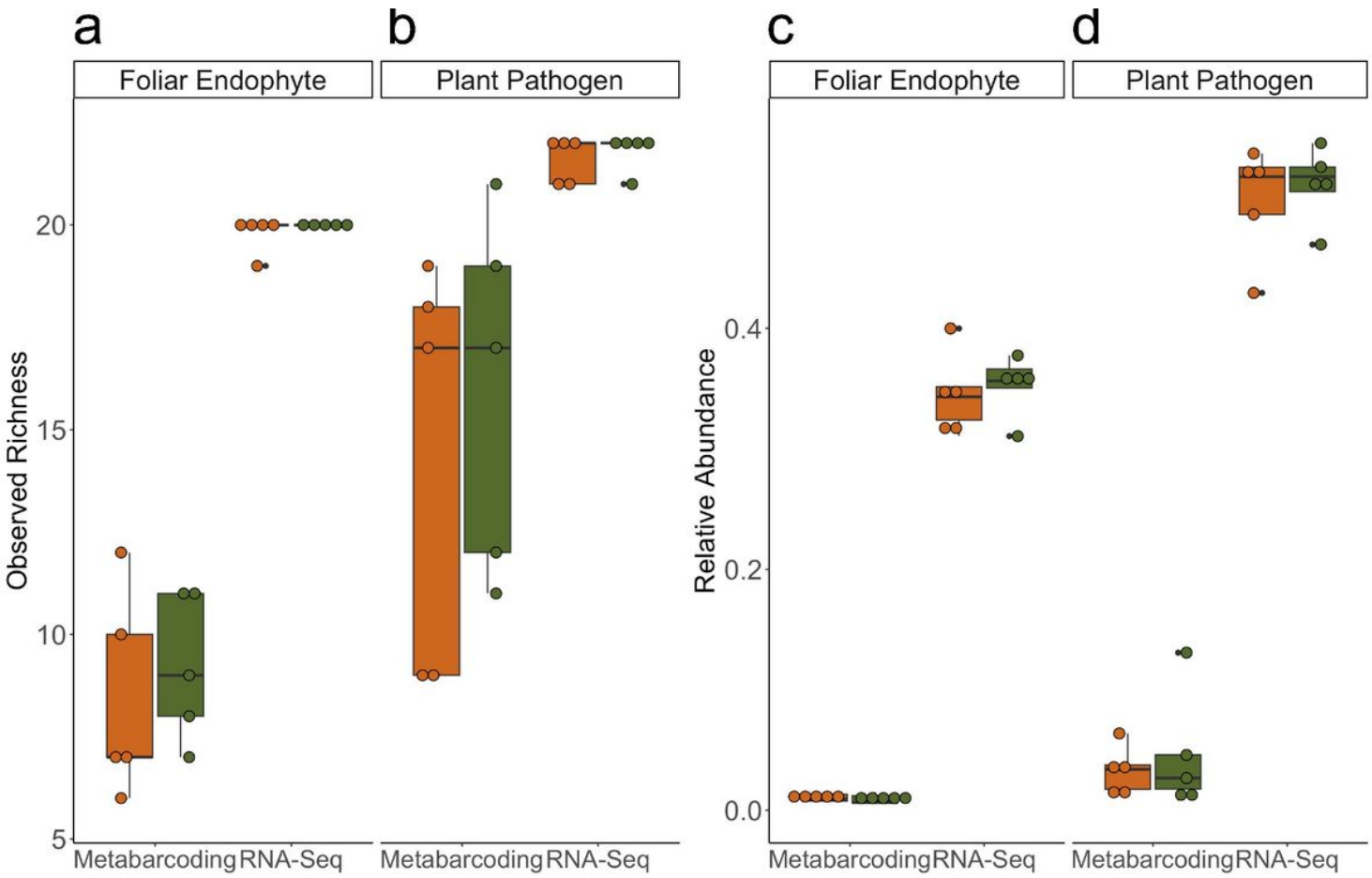

Figure 4

Community composition of foliar endophytes and plant pathogens within the endophyte community of symptomatic and asymptomatic needles according to ITS2 metabarcoding and RNA-seq metatranscriptomics. **a** Observed richness of foliar endophytes. **b** Observed richness of plant pathogens. **c** Relative abundance of foliar endophytes. **d** Relative abundance of plant pathogens

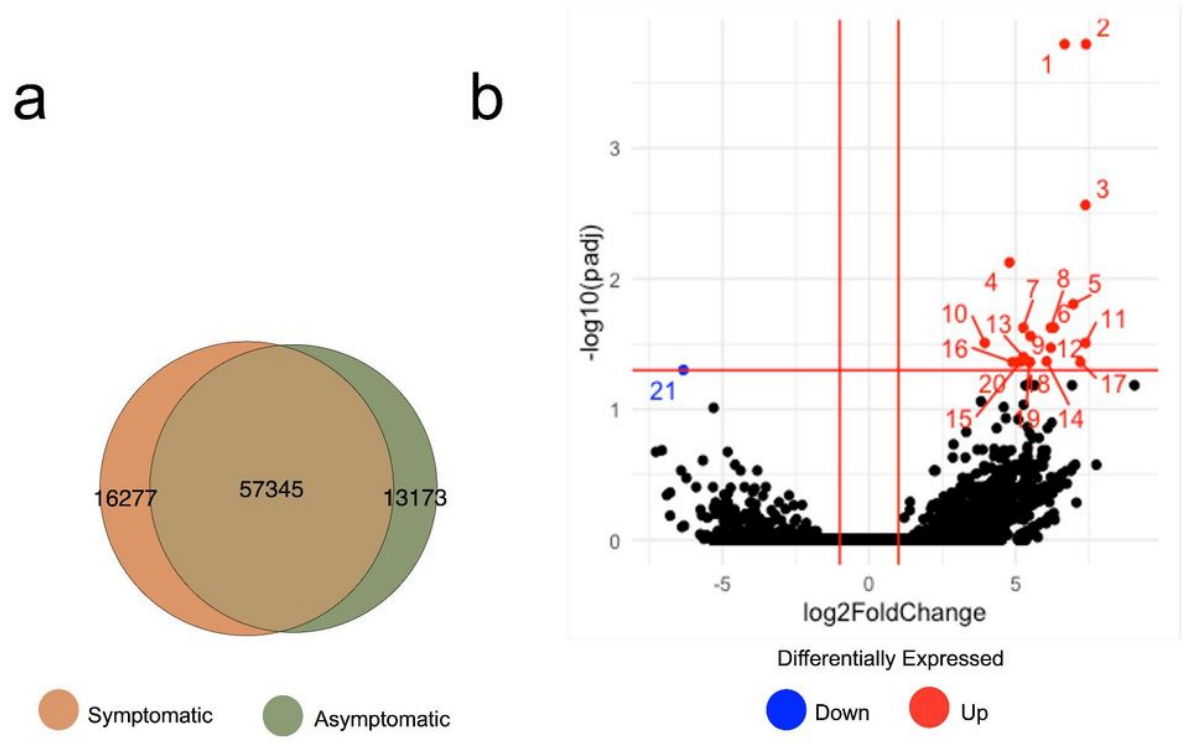

Figure 5

Differential expression of fungal ORFs in asymptomatic and symptomatic needles**. a** Venn diagrams illustrating the number of shared and unique fungal annotated ORFs between host conditions. **b** Volcano plot showing how differentially expressed ORFs were selected according to their log_2FoldChange and adjusted *p-value* (<0.05). Red dots indicate fungal ORFs that are upregulated in asymptomatic needles, while blue dots indicate fungal ORFs that are downregulated in asymptomatic needles compared to those in symptomatic needles. Horizontal red lines depict adjusted *p values (*< 0.05) and vertical red lines indicate the threshold of log_2FoldChange indicating downregulation (< -1) or upregulation (>1)

Supplementary Files

This is a list of supplementary files associated with this preprint. Click to download.

- Supplementalinformation.docx